

Antikaon absorption in nuclear medium and kaonic atoms

Jaroslava Óbertová

*Faculty of Nuclear Sciences and Physical Engineering,
Czech Technical University in Prague*

Àngels Ramos

University of Barcelona

Eliahu Friedman

Hebrew University, Jerusalem

Jiří Mareš

NPI, Řež



ROCKSTAR workshop, 9 - 13 October 2023, Trento, Italy

K^-N interaction

- K^-N interaction near threshold described by chiral coupled-channel interaction models
 - A. Cieply, J. Smejkal, *NPA* 881 (2012) 115 - Prague (P)
 - Y. Ikeda, T. Hyodo, W. Weise, *NPA* 881 (2012) 98 - Kyoto-Munich (KM)
 - A. Feijoo, V. Magas, A. Ramos, *PRC* 99 (2019) 035211 - Barcelona (BCN)
 - Z. H. Guo, J. A. Oller, *PRC* 87 (2013) 035202 - Murcia (M1 and M2)
 - M. Mai, U.-G. Meißner, *NPA* 900 (2013) 51 - Bonn (B2 and B4)
- Info about K^-N interaction below threshold provided by kaonic atoms
65 data points (energy shifts, widths, yields=upper level widths) from CERN, Argonne, RAL, BNL
- Chirally motivated models fail to describe kaonic atom data
E. Friedman, A. Gal, NPA 959 (2017) 66

Multinucleon processes

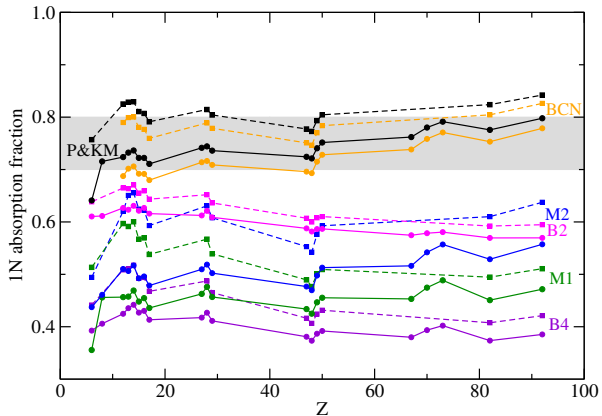
- Chiral models include only $K^- N \rightarrow \pi Y$ ($Y = \Lambda, \Sigma$) decay channel
- K^- interactions with two and more nucleons should be included, (e.g., $K^- + N + N \rightarrow Y + N$) ← analysis of kaonic atom data
E. Friedman, A. Gal, NPA 959 (2017) 66

$$V_{K^-\text{multiN}}^{\text{phen}} = -4\pi B \left(\frac{\rho}{\rho_0}\right)^\alpha \rho ,$$

where B is a complex amplitude, ρ is nuclear density distribution, ρ_0 is saturation density and α is positive

- equally good description of data with $\chi^2/\text{d.p} \leq 2$

Single- vs. multi-nucleon processes

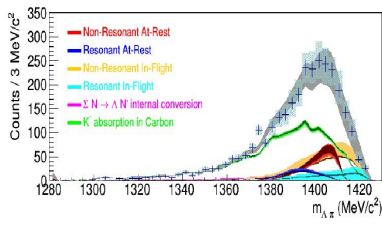


- Fraction of *single-nucleon* absorption 0.75 ± 0.05 (average value) used as an **additional constraint**.

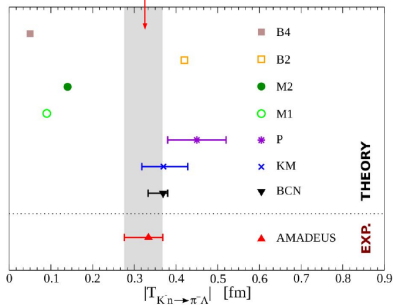
→ Only P, KM and BCN models found acceptable in kaonic atom analysis
E. Friedman, A. Gal, NPA 959 (2017) 66

K. Piscicchia, talk at THEIA-STRONG2020 Web-Seminar, 20 December 2020

Outcome of the measurement

Investigated using: $K^- "n" ^3\text{He} \rightarrow \Lambda\pi^- ^3\text{He}$ 

$$|f_{ar}^s| = (0.334 \pm 0.018 \text{ stat}^{+0.034}_{-0.058} \text{ syst}) \text{ fm}.$$



[K. Piscicchia, S. Wycech, L. Fabbietti et al. Phys.Lett. B782 (2018) 339-345]

[K. Piscicchia, S. Wycech, C. Curceanu, Nucl. Phys. A 954 (2016) 75-93]

Multinucleon porcesse

- K^- multi-nucleon absorption in the surface region of atomic nuclei represents about 20%
NC 53 (1968) 313 (Berkeley), NPB 35 (1971) 332 (BNL), NC 39A (1977) 538 (CERN)
- K^- multi-nucleon absorption in atoms described by phenomenological optical potential
E. Friedman, A. Gal, NPA 959 (2017) 66
- Model for K^-NN absorption in nuclear matter using free-space chiral amplitudes
T. Sekihara et al., PRC 86 (2012) 065205
- New experimental data on K^-NN absorption (AMADEUS@DAΦNE)
K. Piscicchia et al., PLB 782 (2018) 339
R. Del Grande et al., EPJ C79 (2019) 190
- Solid microscopic model for K^-NN absorption needed!

Microscopic model for K^-NN absorption in nuclear matter

Microscopic model for K^- two-nucleon absorption in symmetric nuclear matter *J. Hrtáková, Á. Ramos, PRC 101 (2020) 035204*

- based on a meson-exchange approach
H. Nagahiro et al., PLB 709 (2012) 87
- P and BCN chiral K^-N amplitudes employed
- **Pauli correlations** in the medium for K^-N amplitudes considered
- **real part of the K^-NN optical potential** evaluated as well
- K^-N optical potential derived within the same approach

$K^- N$ absorption in nuclear matter

$$K^- N \rightarrow \pi Y \quad (Y = \Lambda, \Sigma)$$

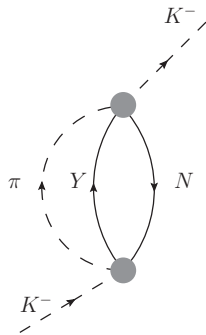
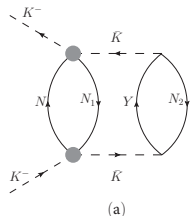


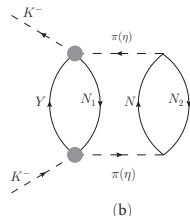
Fig.1: Feynman diagram for K^- absorption on a single nucleon in nuclear matter. The shaded circles denote the $K^- N$ t-matrices derived from a chiral model.

$K^- NN$ absorption in nuclear matter

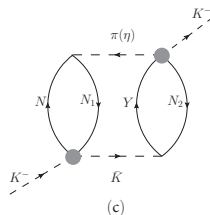
$$K^- + N + N \rightarrow Y + N \quad (Y = \Lambda, \Sigma)$$



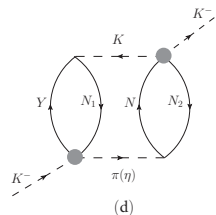
(a)



(b)



(c)



(d)

Fig.2: Two-fermion-loop (2FL) Feynman diagrams for non-mesonic K^- absorption on two nucleons N_1 , N_2 in nuclear matter. The shaded circles denote the K^-N t-matrices derived from a chiral model.

$K^- NN$ absorption in nuclear matter

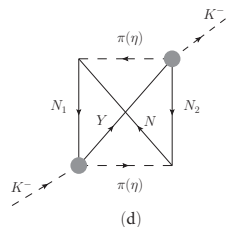
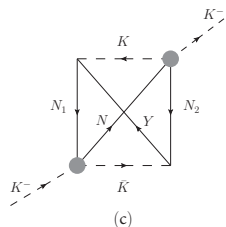
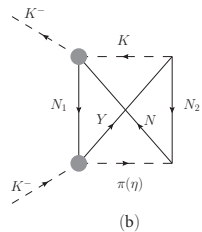
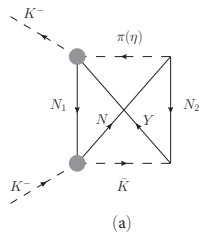


Fig.3: One-fermion-loop (1FL) Feynman diagrams for non-mesonic K^- absorption on two nucleons N_1 , N_2 in nuclear matter. The shaded circles denote the $K^- N$ t-matrices derived from a chiral model.

$K^- NN$ absorption in nuclear matter

- $V_{K^- N} = \sum_{\text{channels}} V_{K^- N \rightarrow \pi Y}$ (Fig.1)
- $V_{K^- NN} = \sum_{\text{channels}} V_{K^- NN}^{\text{2FL}} + V_{K^- NN}^{\text{1FL}}$ (Fig.2 and 3)
→ contributions from 37 2FL and 28+33 1FL diagrams

Table 2: All considered channels for mesonic and non-mesonic K^- absorption in matter.

$K^- N \rightarrow \pi Y$		$K^- N_1 N_2 \rightarrow Y N$	
$K^- p$	$\rightarrow \pi^0 \Lambda$ $\rightarrow \pi^0 \Sigma^0$ $\rightarrow \pi^+ \Sigma^-$ $\rightarrow \pi^- \Sigma^+$	$K^- pp$	$\rightarrow \Lambda p$ $\rightarrow \Sigma^0 p$ $\rightarrow \Sigma^+ n$
$K^- n$	$\rightarrow \pi^- \Lambda$ $\rightarrow \pi^- \Sigma^0$ $\rightarrow \pi^0 \Sigma^-$	$K^- pn(np)$	$\rightarrow \Lambda n$ $\rightarrow \Sigma^0 n$ $\rightarrow \Sigma^- p$
		$K^- nn$	$\rightarrow \Sigma^- n$

AMADEUS: Ratio for 2N absorption

Recently measured ratio *R. Del Grande et al., EPJ C79 (2019) 190*

$$R = \frac{\text{BR}(K^- pp \rightarrow \Lambda p)}{\text{BR}(K^- pp \rightarrow \Sigma^0 p)} = 0.7 \pm 0.2(\text{stat.})^{+0.2}_{-0.3}(\text{syst.})$$

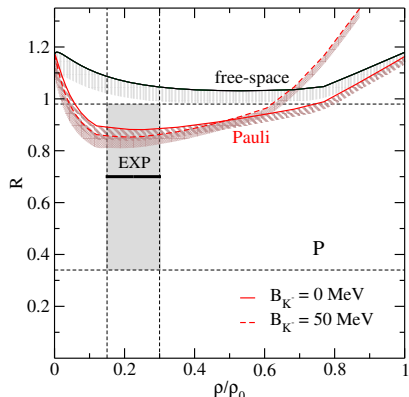
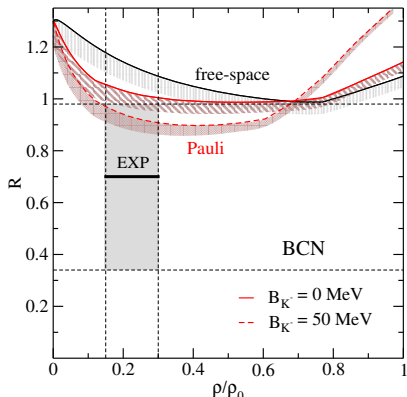


Fig.4: The ratio R as a function of relative density, calculated using the free-space and Pauli blocked amplitudes for $B_{K^-} = 0$ MeV and $B_{K^-} = 50$ MeV. Color bands denote the uncertainty due to different cut-off values $\Lambda_c = 800 - 1200$ MeV.

Application to kaonic atoms

J. Őbertová, E. Friedman, J. Mareš, PRC 106 (2022) 065201

- K^-NN model applied in calculations of energy shifts and widths in kaonic atoms
- BCN amplitudes used → in-medium modifications included
(Pauli or WRW *T. Wass, M. Rho, W. Weise, NPA 617 (1997) 449*)
- microscopic $K^-N + K^-NN$ potentials calculated for 23 targets and confronted with kaonic atom data
- $K^-N + K^-NN$ potentials then supplemented by a phenomenological term describing 3 and 4 nucleon processes $\sim -4\pi B(\frac{\rho}{\rho_0})^\alpha \rho$
- values of α and complex amplitude B fitted to data

Kaonic atoms calculations

Table 3: Values of χ^2 for shifts, widths and yields in selected K^- atoms, calculated with K^-N , $K^-N + K^-NN$ and $K^-N+\text{phen. multiN}$ potentials based on BCN Pauli or WRW modified amplitudes. Experimental data are shown for comparison.

BCN		WRW		Pauli		phen.	EXP
		K^-N	$+K^-NN$	K^-N	$+K^-NN$	$K^-N + \text{phen. multiN}$	
C^{12}	$\Delta(\epsilon)$	101.52	34.35	25.13	11.48	1.76	-0.59 (0.08)
	Γ	44.80	27.45	17.00	9.44	0.70	1.73 (0.15)
	Γ^*	1.71	1.47	0.15	0.67	2.74	0.99 (0.20)
P^{31}	$\Delta(\epsilon)$	41.04	15.13	10.46	6.35	0.03	-0.33 (0.08)
	Γ	13.72	10.34	11.43	6.42	0.24	1.44 (0.12)
	Γ^*	5.17	4.70	5.98	1.87	0.30	1.89 (0.30)
S^{32}	$\Delta(\epsilon)$	475.71	209.40	90.77	80.82	1.24	-0.494 (0.038)
	Γ	0.76	2.83	67.35	43.29	9.24	2.19 (0.10)
	Γ^*	13.32	10.85	9.45	2.78	0.47	3.03 (0.44)
C^{35}	$\Delta(\epsilon)$	38.27	17.69	4.23	4.62	2.10	-0.99 (0.17)
	Γ	5.94	2.56	10.94	5.39	0.00	2.91 (0.24)
	Γ^*	7.92	4.53	2.27	0.74	0.15	5.8 (1.70)
Cu^{63}	$\Delta(\epsilon)$	33.50	8.93	1.54	2.71	3.19	-0.370 (0.047)
	Γ	0.31	0.02	4.90	3.57	2.25	1.37 (0.17)
	Γ^*	0.98	0.13	0.24	0.73	1.52	5.2 (1.1)
Sn^{118}	$\Delta(\epsilon)$	9.00	8.81	6.57	8.50	2.15	-0.41 (0.18)
	Γ	0.42	0.03	0.35	0.71	0.29	3.18 (0.64)
	Γ^*	24.53	15.08	5.04	4.80	4.09	15.1 (4.4)
Pb^{208}	$\Delta(\epsilon)$	7.52	3.67	3.24	4.84	0.34	-0.02 (0.012)
	Γ	0.12	0.10	0.31	0.38	0.39	0.37 (0.15)
	Γ^*	0.06	0.18	0.35	0.41	0.52	4.1 (2)
χ^2	total	820.37	378.24	277.69	200.54	33.71	
	S^{32}_{out}	330.58	155.16	110.13	73.65	22.76	

Calculated branching ratios in $^{12}\text{C} + \text{K}^-$ atom

Table 4: Primary-interaction branching ratios (in %) for mesonic ($K^- N \rightarrow Y\pi$, $Y = \Lambda, \Sigma$) and non-mesonic absorption ($K^- NN \rightarrow YN$) of K^- in $^{12}\text{C} + \text{K}^-$ atom ($|l|=2$), calculated with $K^- N + K^- NN$ potentials based on WRW and Pauli blocked BCN and P amplitudes. The experimental data corrected for primary interaction are shown for comparison.

$^{12}\text{C} + \text{K}^-$ ($ l =2$)	BCN		P		Exp. ^{12}C [1]
	WRW	Pauli	WRW	Pauli	
$\Sigma^+ \pi^-$	26.9	22.4	28.1	22.1	29.4 ± 1.0
$\Sigma^- \pi^0$	8.3	7.7	7.2	5.9	2.6 ± 0.6
$\Sigma^- \pi^+$	15.5	17.5	17.1	17.6	13.1 ± 0.4
$\Sigma^0 \pi^-$	8.4	7.9	7.3	5.9	2.6 ± 0.6
$\Sigma^0 \pi^0$	17.2	16.4	19.3	17.3	20.0 ± 0.7
$\Lambda \pi^0$	5.2	5.0	4.2	3.7	3.4 ± 0.2
$\Lambda \pi^-$	10.4	9.9	8.3	7.2	6.8 ± 0.3
total 1N ratio	91.9	87.0	90.7	82.0	77.9 ± 1.6
non-mesonic ratio	WRW	Pauli	WRW	Pauli	76% $\text{CF}_3\text{Br} + 24\% \text{C}_3\text{H}_8$ [2]
$\Lambda p + \Lambda n + \Sigma^0 p + \Sigma^0 n$	4.2	6.7	4.6	9.0	$14.1 \pm 2.5^{\text{a}}$
$\Sigma^- p + \Sigma^- n$	1.7	3.1	2.1	4.2	$7.3 \pm 1.3^{\text{a}}$
$\Sigma^+ n$	2.2	3.5	2.6	4.8	$4.3 \pm 1.2^{\text{a}}$
$\Sigma^0 p + \Sigma^0 n$	1.9	3.1	2.2	4.2	-
total 2N ratio	8.1	13.0	9.3	18.0	$16 \pm 3(\text{stat.})^{+4}_{-5}(\text{syst.})$ [3]

^a multinucleon capture rate

[1] C. Vander Velde-Wilquet et al., NC 39 A (1977) 538

[2] H. Davis et al., NC 53 A (1968) 313

[3] R. Del Grande et al., EPJ C79 (2019) 190

Confrontation with kaonic atom data

Table 5: Values of $\chi^2(65)$ resulting from comparisons of predictions with kaonic atom data using K^-N , $K^-N + K^-NN$, and $K^-N + K^-NN + \text{phen. multiN}$ potentials. Values of complex amplitude B and parameter α for potentials based on Pauli blocked and WRW modified BCN amplitudes.

	K^-N	$K^-N + K^-NN$	+ phen.	$\text{Re}B$ (fm)	$\text{Im}B$ (fm)	α
Pauli	825	565	105	-1.97(13)	-0.93(11)	1.4
WRW	2378	1123	116	-0.90(9)	0.72(10)	0.6

- best fit $K^-N + \text{phen. multiN}$ potential based on BCN amplitudes
 $\text{Re}B = -1.3$ fm, $\text{Im}B = 1.9$ fm, $\alpha = 1$, $\chi^2 = 112.3$

Hadron self-energies

- inclusion of Y , N , K^- and π self-energies into the K^-N chiral BCN amplitudes as well as into the K^-NN model.
- we considered following baryon potentials

$$V_N = -50 \frac{\rho}{\rho_0} ,$$

$$V_\Lambda = -340\rho + 1087.5\rho^2 \rightarrow V_\Lambda(\rho_0) = -26.4 \text{ MeV},$$

$$V_\Sigma = 30 \frac{\rho}{\rho_0} .$$

- we considered pion S- and P-wave self-energy

A. Ramos, E. Oset, NPA 671 (2000) 481

Hadron self-energies: $K^- p$ amplitudes

Preliminary results

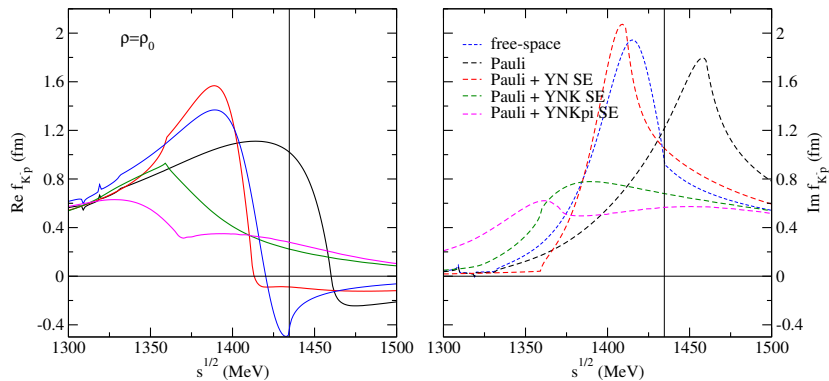


Fig.5: Comparison of $K^- p \rightarrow K^- p$ BCN amplitudes with Pauli blocking only (black), Pauli+YN SE (red), Pauli + YNK^- SE (green), and Pauli + $YNK^- \pi$ SE (magenta) at saturation density ρ_0 .

Hadron self-energies: $K^- n$ amplitudes

Preliminary results

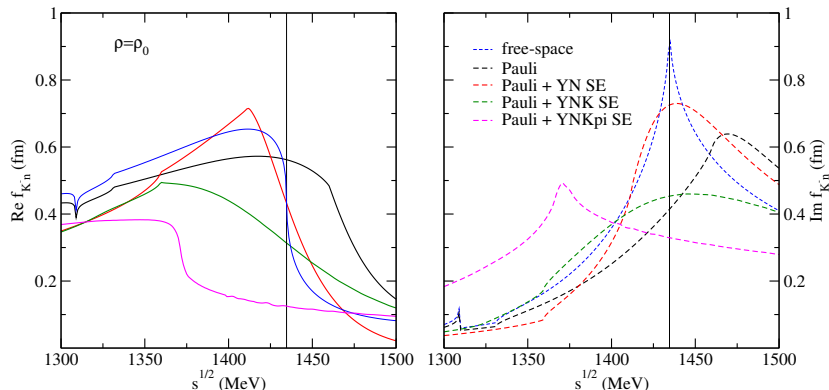


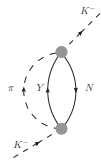
Fig.6: Comparison of $K^- n \rightarrow K^- n$ BCN amplitudes with Pauli blocking only (black), Pauli+YN SE (red), Pauli + YNK⁻ SE (green), and Pauli + YNK⁻ π SE (magenta) at saturation density ρ_0 .

Hadron self-energies: K^- potential

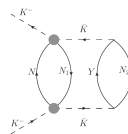
- Pauli + YN SE amplitudes $\Rightarrow V_{K^-} = V_{K-N} + V_{K-NN}$
- Pauli + $YNK^-(YNK^-\pi)$ SE amplitudes



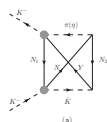
$$V_{K^-} = t\rho + V_{K-NN}^{\text{corr}}$$



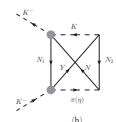
$+$



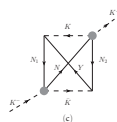
$+ \dots +$



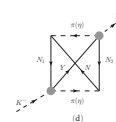
(a)



(b)



(c)



(d)

Hadron self-energies: total K^- potential

Preliminary results

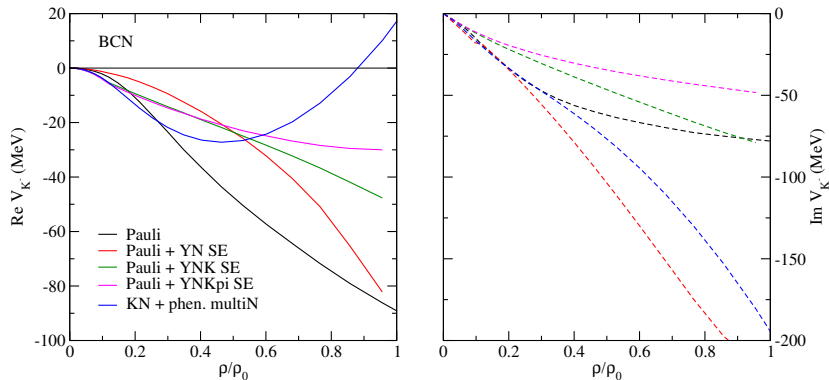


Fig.7: Real (left) and imaginary (right) parts of the total K^- potential as a function of relative density ρ/ρ_0 , calculated with Pauli, Pauli + YN SE, Pauli + YNK^- SE, and Pauli + $YNK^- \pi$ SE BCN amplitudes. For comparison there is the best fit $K^- N +$ phen. multiN potential based on BCN amplitudes (blue).

Branching ratios for mesonic and non-mesonic absorption

Table 6: Primary-interaction ratios (in %) for mesonic and non-mesonic absorption of K^- in nuclear matter, calculated with Pauli blocked and Pauli + YN self-energies amplitudes in the BCN model. The experimental data corrected for primary interaction are shown for comparison.

BCN	0.3 ρ_0		Exp. [1]	
mesonic ratio	Pauli	Pauli+YN se	^4He	^{12}C
$\Sigma^+\pi^-/K^-$	28.8 ± 0.7	22.6 ± 0.7	31.2 ± 5.0	29.4 ± 1.0
$\Sigma^-\pi^0/K^-$	5.7 ± 0.1	5.4 ± 0.2	4.9 ± 1.3	2.6 ± 0.6
$\Sigma^-\pi^+/K^-$	14.8 ± 0.4	19.6 ± 0.6	9.1 ± 1.6	13.1 ± 0.4
$\Sigma^0\pi^-/K^-$	5.7 ± 0.1	5.4 ± 0.2	4.9 ± 1.3	2.6 ± 0.6
$\Sigma^0\pi^0/K^-$	19.2 ± 0.5	18.9 ± 0.6	17.7 ± 2.9	20.0 ± 0.7
$\Lambda\pi^0/K^-$	3.5 ± 0.1	3.8 ± 0.1	5.2 ± 1.6	3.4 ± 0.2
$\Lambda\pi^-/K^-$	7.0 ± 0.2	7.7 ± 0.2	10.5 ± 3.0	6.8 ± 0.3
total 1N ratio	84.6 ± 2.2	83.4 ± 2.4	83.5 ± 7.1	77.9 ± 1.6
non-mesonic ratio	Pauli	Pauli+YN se	76% $\text{CF}_3\text{Br} + 24\%$ C_3H_8 [2]	
$(\Lambda p + \Lambda n + \Sigma^0 p + \Sigma^0 n)/K^-$	7.2 ± 1.1	7.9 ± 1.2	$14.1 \pm 2.5^{\text{a}}$	
$(\Sigma^- p + \Sigma^- n)/K^-$	4.3 ± 0.6	5.6 ± 0.8	$7.3 \pm 1.3^{\text{a}}$	
$\Sigma^+ n/K^-$	3.8 ± 0.5	3.2 ± 0.4	$4.3 \pm 1.2^{\text{a}}$	
$(\Sigma^0 p + \Sigma^0 n)/K^-$	3.7 ± 0.5	4.0 ± 0.7	-	
total 2N ratio	15.4 ± 2.2	16.6 ± 2.4	$16 \pm 3(\text{stat.})^{+4}_{-5}(\text{syst.})$ [3]	

^a multinucleon capture rate

[1] C. Vander Velde-Wilquet et al., NC 39 A (1977) 538

[2] H. Davis et al., NC 53 A (1968) 313

[3] R. Del Grande et al., EPJ C79 (2019) 190

Summary

- K^-N interaction described by chiral meson-baryon coupled channel interaction models
- Chiral models are unable to describe kaonic atom data
- Interactions of K^- with two and more nucleons important for realistic description of the K^- -nucleus interaction
 - ▶ only P, KM, and BCN models compatible with available data

Summary

- We have developed a microscopic model for K^-NN absorption in nuclear matter using amplitudes derived from the P and BCN chiral meson-baryon interaction models

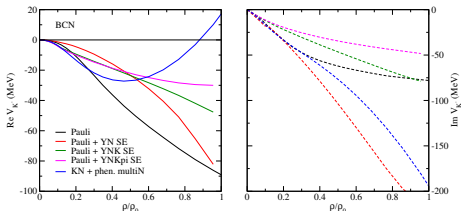
J. Hrtáková, Á. Ramos, PRC 101 (2020) 035204

- ▶ Pauli blocked amplitudes included → medium effects non-negligible
- Microscopic $K^-N + K^-NN$ potentials confronted with kaonic atom data *J. Őbertová, E. Friedman, J. Mareš, PRC 106 (2022) 065201*
 - ▶ the description of kaonic atoms improves considerably when microscopic K^-NN potentials are included (χ^2 drops down twice)
 - ▶ microscopic $K^-N + K^-NN$ potentials still have to be supplemented by a phenomenological term to account for K^-3N (4N) processes and to get $\chi^2/d.p. \leq 2$
- Further improvements of the K^-NN model → inclusion of hadron self-energies in progress!

Summary on Antikaon absorpiton in nuclear matter

- K^- -single nucleon potentials based on chiral amplitudes fail to describe the kaonic atom data
- microscopic model for the K^-NN absorption in medium developed using the chiral K^-N amplitudes with Pauli blocking
- the model was successfully applied in kaonic atoms calculations

	K^-N	$K^-N + K^-NN$	+ phen.	$\text{Re}B$ (fm)	$\text{Im}B$ (fm)	α
Pauli	825	565	105	-1.97(13)	-0.93(11)	1.4
WRW	2378	1123	116	-0.90(9)	0.72(10)	0.6



- further improvement of the model in progress: proper inclusion of hadron selfenergies in the chiral amplitudes as well as in the K^-NN model
- total K^- potential in nuclear matter derived as a function of density